Analysis of a New Workspace of the Hexaglide as a Motion Simulator for Fuel Tanker Trucks

Minxiu Kong, Yong Zhang*, Lining Sun and Zhijiang Du
Robotics Institute, Harbin Institute of Technology, Harbin, China

***Abstract*— The Hexaglide is a 6-DOF fully parallel mechanism characterized by six length-constant legs and three parallel guide rails. The application of this architecture for simulating the motions of fuel tanker trucks is firstly presented. The kinematic model of the simulator is established, the inverse kinematics is analyzed, and the kinematic constraints are summarized. Then a new type of workspace called the position workspace with a specified orientation requirement is proposed, which takes into account the strong coupling between position workspace and orientation workspace. And two approaches to obtaining this workspace are also developed and demonstrated by the preliminary workspace analysis of the simulator.**

***Index Terms*— Hexaglide, motion simulator, kinematics, workspace.**

I. Introduction

To test the performance of various sensors installed on fuel tanker trucks, such as pressure sensors, gas sensors, acceleration sensors, obliquity sensors, liquid level meters and door switches, these sensors should be carried by real fuel tanker trucks which have to be driven under various conditions, such as rough roads, long hours, hard braking, sharp turning, relatively high and low temperatures, gas leakage and even crashes. This test method not only need experienced drivers and may be harmful to them, but also is inaccurate, which results in unreliable test results.

In view of these disadvantages of the field test, the construction of a simulation system is considered for testing and measuring the essential performance indexes of the sensors. This research is mainly composed of three parts, namely, the modeling of work conditions, the development of a motion simulator, and the study of a test system. This paper deals with the second part, and mainly concerns the workspace analysis of the simulator.

First of all, the kinematic structure (or type) of the simulator should be determined, which should satisfy all the requirements listed as follows.

1) To simulate the real test conditions aforementioned, the simulator should provide the motions of six degrees of freedom.
2) The acceleration is fairly high ($14 m/s^2$) when the truck starts up and brakes in emergencies, so the simulator should be capable of providing large acceleration along one axis. Besides, to assure sufficient duration of acceleration, the simulator should have long strokes along that maximum-acceleration direction.
3) The simulator should be compact enough to be easily placed in a standard sealed room which is mainly intended for the simulation of temperatures and the leakage of several harmful gases.
4) The field test requires long road hauls on rough road surfaces, which causes frequent vertical vibrations (30Hz) of the truck. Thereby the simulator should have large bandwidth in the vertical direction.

In consideration of the above requirements, it is suitable or even necessary to utilize a 6-DOF fully parallel mechanism for this occasion. Parallel mechanisms have been extensively studied over the last thirty years, and the readers are referred to [1] and [2] for detailed reviews on parallel robots. In a nutshell, the advantages of parallel mechanisms over serial ones are their larger load-to-weight ratio, higher structural rigidity, and better dynamic performance.

There are several types of fully parallel mechanisms, and the most prestigious one is the Stewart-Gough platform [3]. Among these existing architectures, the Hexaglide is chosen due to its favorable performance concerning acceleration in one direction. As shown in Fig. 1, it is composed of a top plate (1), six length-constant links (2), six sliders (3), three linear guide rails (4), and six linear actuators (5). Each of the six links is attached to the top plate through a ball-in-socket spherical joint providing three rotational DOFs, and the corresponding slider through a universal joint with two rotational DOFs. In addition, there is a translational DOF between each slider and its corresponding rail. Thus each subchain has six degrees of freedom. The top plate, links and sliders can move along rails as a whole without relative motions among one another, and hence the top plate can attain the maximum acceleration of the actuators if speed reducers are not used. Furthermore, the length of rails can be freely chosen according to the need of acceleration duration.

The concept of the Hexaglide was first developed by the Institute of Machine Tools of Swiss Federal Institute of Technology Zurich [4], for designing a high speed milling machine, and then [5] and [6] discussed the relevant control issues. Besides, a safety-enhanced surgical robot [7] has been proposed based on the Hexaglide architecture.

It is well-known that the position workspace and orientation workspace of 6-DOF parallel mechanisms are strongly coupled. Therefore, their full workspace is 6 dimensional, which makes it difficult for graphical representation. And there has been scarce work addressing this problem. Merlet [8] presented a method for detecting whether straight line paths with constant orientation or varying orientation is contained in

*Corresponding author. Phone: +86-451-86414462 ext 21; Fax: +86-451-86414174; Email: zhangyong212@hit.edu.cn.

1-4244-1184-X/07/$25.00©2007 IEEE

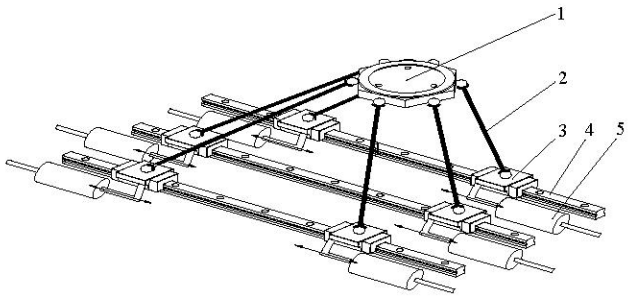

Fig. 1. Hexaglide.

the workspace. Gosselin [9] presented a discretization method for the computation and graphical representation of a new workspace with coupled translational and rotational DOFs.

In this paper, a new type of workspace comprising of all attainable positions with a range of orientation requirements is proposed in Section IV, following the preparation of the kinematic analysis and kinematic constraint summary in Section II and III, respectively. And finally the conclusions are given in Section V.

II. Kinematic Analysis

A. Kinematic Model

The mobility M of the parallel mechanism under study can be determined by applying the Chebyshev-Grübler-Kutzbach formula, i.e.,

$$M = 6(b - g - 1) + \sum_{k} f_k \tag{1}$$

where b and g are, respectively, the number of bodies (including the base) and the number of the joints of the mechanism, and f_k is the number of DOFs of joint k. Given the particular topological structure of the mechanism, we have $b = 14$, $g = 18$, and $\sum_k f_k = 36$, the mobility M of the mechanism thus being equal to six. Correspondingly, this 6-DOF mechanism is actuated by a set of six input displacements, s_i, for $i = 1 - 6$.

To perform the kinematic analysis of the Hexaglide, the coordinate systems are established, as shown in Fig. 2. And to give the maximum symmetry to the mechanism, the gaps between the adjacent rails are the same (denoted by λ), the lengths of the six links (denoted by $l_1, l_2, \ldots, l_6$) are all l, the top plate is a regular hexagon and the spherical joints are located at its vertexes.

B. Inverse Kinematic Analysis

The Inverse kinematics computes the locations of the six sliders given the position and orientation $(x, y, z, \phi, \theta, \psi)$ of the top plate. The position P_i of a spherical joint can be represented by using (4×4) homogeneous matrices in the global reference frame as

$$P_i = T(x, y, z)R(\phi, \theta, \psi)R_z(\delta_i)T_x(r)[0, 0, 0, 1]^T \tag{2}$$

where the homogeneous matrices $T(x, y, z)$ and $R(\phi, \theta, \psi)$, respectively, specifies the translation of the top plate origin and

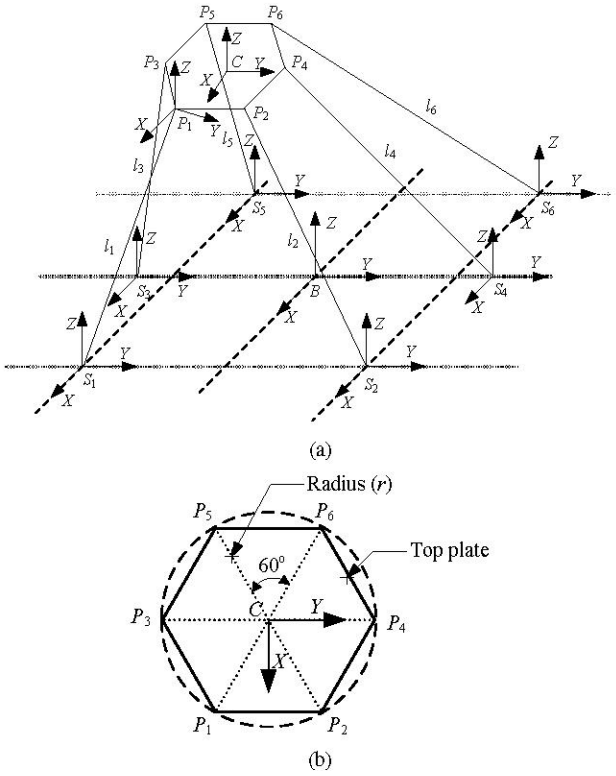

Fig. 2. Kinematic model. (a) Coordinate system establishment. (b) Top plate.

the orientation of the top plate. Given the position coordinate (x, y, z) of the top plate origin in respect to the global frame, the form of the translation matrix $T(x, y, z)$ is determined and can only be expressed as

$$T(x, y, z) = \begin{bmatrix} 1 & 0 & 0 & x \\ 0 & 1 & 0 & y \\ 0 & 0 & 1 & z \\ 0 & 0 & 0 & 1 \end{bmatrix}. \tag{3}$$

Nonetheless, the form of the orientation matrix can not be determined only by the orientation of the top plate. In other words, given a specified orientation of the top plate, the set of angles (ϕ, θ, ψ), which are referred to as Euler angles, are not unique. In accordance to different rotating sequences, there are different sets of Euler angles, two of which are recalled here since they will be used later for the workspace analysis.

Conventionally, the orientation of the top plate is represented by the ZXY Euler angles, which are defined by first rotating the mobile frame about the base z_b axis by an angle ϕ, then about the new x_p axis by an angle θ, and finally about the new y_p axis by an angle ψ. For this choice of Euler angles, the singularity occurs at $\theta = \pm\pi/2$ and the rotation matrix is defined as

$$\begin{aligned} R &= R_z(\phi)R_x(\theta)R_y(\psi) \\ &= \begin{bmatrix} \mathrm{c}_\phi\mathrm{c}_\psi - \mathrm{s}_\phi\mathrm{s}_\theta\mathrm{s}_\psi & -\mathrm{s}_\psi\mathrm{c}_\theta & \mathrm{c}_\phi\mathrm{s}_\psi + \mathrm{s}_\phi\mathrm{s}_\theta\mathrm{c}_\psi & 0 \\ \mathrm{s}_\phi\mathrm{c}_\psi + \mathrm{c}_\phi\mathrm{s}_\theta\mathrm{s}_\psi & \mathrm{c}_\phi\mathrm{c}_\theta & \mathrm{s}_\phi\mathrm{s}_\psi - \mathrm{c}_\phi\mathrm{s}_\theta\mathrm{c}_\psi & 0 \\ -\mathrm{c}_\theta\mathrm{s}_\psi & \mathrm{s}_\theta & \mathrm{c}_\theta\mathrm{c}_\psi & 0 \\ 0 & 0 & 0 & 1 \end{bmatrix} \end{aligned} \tag{4}$$

where $c_\phi \equiv \cos\phi$, $c_\psi \equiv \cos\psi$, $s_\phi \equiv \sin\phi$, etc.

Besides, the orientation of the top plate can also be described by a modified set of Euler angles presented by Bonev [10], [11]. The advantages of this set of Euler angles were presented in [12], which applied it to the analysis of constrained manipulators. It was also used in [13] for formulating the closed-form solution to the orientation workspace of Gough-Stewart parallel manipulators. In this orientation representation, the top plate is first rotated about the base z_b axis by an angle ϕ, then about the new y_p axis by an angle θ, and finally about the mobile z_p axis by an angle $\psi - \phi$. For this choice of Euler angles, the singularity occurs at $\theta = 0°$, and the corresponding rotation matrix is given by

$$R = R_z(\phi)R_y(\theta)R_z(\psi-\phi) = \begin{bmatrix} c_\phi c_\theta c_{(\psi-\phi)} & -c_\phi c_\theta s_{(\psi-\phi)} & c_\phi s_\theta & 0 \\ -s_\phi s_{(\psi-\phi)} & -s_\phi c_{(\psi-\phi)} & & \\ s_\phi c_\theta c_{(\psi-\phi)} & -s_\phi c_\theta s_{(\psi-\phi)} & s_\phi s_\theta & 0 \\ +c_\phi s_{(\psi-\phi)} & +c_\phi c_{(\psi-\phi)} & & \\ -s_\theta c_{(\psi-\phi)} & s_\theta s_{(\psi-\phi)} & c_\theta & 0 \\ 0 & 0 & 0 & 1 \end{bmatrix}. \quad (5)$$

This approach for describing orientation is much more intuitive than other sets of Euler angles, with the Euler angles θ and ϕ respectively denoting the zenith angle and azimuth angle of the z_p axis of the top plate in a spherical coordinate system with respect to the global frame. And the Euler angle ψ represents the rotation angle about the mobile z_p axis, referred to as the torsion angle intuitively.

The position S_i of a universal joint can be represented by

$$S_i = [\lambda_i, s_i, 0, 1]^T. \quad (6)$$

In view of the fact that the length of the six legs is constant, the active straight-line displacement can be obtained by solving the following equations.

$$\|P_i - S_i\| = l_i, \quad i = 1, 2, \ldots, 6. \quad (7)$$

For the real-time control, the coordinate (p_{ix}, p_{iy}, p_{iz}) of the point P_i is obtained by solving (2) first, and then the active displacement s_i is given by the following expressions derived from (7).

$$s_i = \begin{cases} p_{iy} - \sqrt{l_i^2 - (p_{ix}-\lambda)^2 - p_{iz}^2}, & i = 1, 3, 5 \\ p_{iy} + \sqrt{l_i^2 - (p_{ix}-\lambda)^2 - p_{iz}^2}, & i = 2, 4, 6. \end{cases} \quad (8)$$

III. Kinematic Constraints

There are various kinematic constraints that may limit the workspace of the Hexaglide. This section models these potential constraints one by one mathematically.

A. Range of Motion of the Universal Joints

It is assumed that at the initial setting, the pose of the top plate is $(0, 0, z_o, 0, 0, 0)$, and all the universal joints and the spherical joints are isotropy in terms of the range of motion in every direction. The initial vector of the link i is denoted by $\boldsymbol{l}_{io}$, and the current vector is denoted by $\boldsymbol{l}_i$. The maximum misalignment angle of the universal joints is denoted by γ_u. Thereby the angle between l_i and l_{io} should be no larger than γ_u, i.e.,

$$\arccos\left(\frac{\boldsymbol{l}_i \cdot \boldsymbol{l}_{io}}{l_i^2}\right) \leqslant \gamma_u. \quad (9)$$

B. Range of Motion of the Spherical Joints

The initial vector of link i is also the initial vector of the symmetrical axis of the socket of the universal joint i. And the sockets are fixed to the to the top plate, and hence have the same rotation matrix as the top plate. The maximum misalignment angle of the universal joints is denoted by γ_s. Thereby,

$$\arccos\left(\frac{\boldsymbol{l}_i \cdot R(\phi,\theta,\psi)\boldsymbol{l}_{io}}{l_i^2}\right) \leqslant \gamma_s. \quad (10)$$

C. Slider Interference

Every pair of the sliders on the same rail should not interfere with each other, taking into account the length of the sliders. This consideration imposes a constraint on the distance between every pair of universal joints, so that

$$s_i - s_{i-1} < d_s, \quad i = 2, 4, 6, \quad (11)$$

where d_s denotes the minimum distance between the two universal joints corresponding to the same rail.

D. Link Interference

It is assumed that the links can be approximated by cylinders of diameter D. The only concern is given to the collision between l_3 and l_1 (or l_5), and l_4 and l_2 (or l_6). Thereby the structure of hexaglides imposes a set of constraints, so that

$$\begin{cases} \text{distance}(l_3, l_1) > D, & \text{distance}(l_3, l_5) > D, \\ \text{distance}(l_4, l_2) > D, & \text{distance}(l_4, l_6) > D. \end{cases} \quad (12)$$

These constraints check equations require the computation of the minimum distance between two line segments, which requires the implementation of a multistep algorithm, which is not recalled due to space limitations. The readers are referred to [14].

E. The Length of The Rails

The strokes of the linear actuators are constrained by the length of the rails. Considering also the length of the sliders, the position the universal joints is constrained by

$$s_i \in \begin{cases} (k_1, k_2), & i = 1, 2, 5, 6 \\ (k_3, k_4), & i = 3, 4, \end{cases} \quad (13)$$

where (k_1, k_2) is the working range of the sliders 1, 2, 5, and 6, and (k_3, k_4) is the working range of the sliders 3 and 4, assuming that the two lateral rails have the same length.

F. Compatibility Constraint

In general, a given configuration of a parallel mechanism may satisfy all the constraints above but still be unattainable from its initial assembly configuration. Since the discretization method is used for obtaining workspace, no direct concern is given to this constraint [14], [15].

G. Additional Mechanical Constraints

The specific design of the prototype imposes to consider the following constraint:

$$z > 0. \tag{14}$$

This consideration avoids the interference between the sliders and the links (or the universal joints).

In addition, in terms of the y_b direction, a pair of universal joints corresponding to the same rail should not enter the area between between the corresponding pair of the spherical joints, i.e.,

$$\begin{cases} s_i < p_{iy}, & i = 1, 3, 5 \\ s_i > p_{iy}, & i = 2, 4, 6. \end{cases} \tag{15}$$

IV. Workspace with Specified Orientation Capabilities

This section presents two methods for the determination of all the possible locations of the center of the top plate so that it is possible to have any orientation of the top plate within some prescribed ranges for the orientation angles. Corresponding to two separate sets of Euler angles aforementioned, two methods are presented.

A. Workspace Without Orientation Requirement

The workspace is obtained by searching for its boundaries in a cylinder coordinate system, which is shown in Fig. 3(a), using the method proposed in [16]. Without the consideration of the rail length constraint, the XZ cross-sections of the workspace are congruent, as shown in Fig. 3(b). Therefore, the workspace analysis is reduced to the analysis of a planar cross-section, the boundary of which can be searched for in a polar coordinate system. This feature also means that the workspace analysis of a general Hexaslide (including HexaM [17], [18], Hexapod [19] and Hexaglide) by Rao in [20] and [**?**] does not apply to the Hexaglide.

B. Using Conventional ZXY Euler Angles with Orientation Requirement as a Rectangular Solid

The orientation requirement can be represented by a rectangular solid in a Cartesian coordinate system, which is expressed by the following set and shown in Fig. 4.

$$W_r = \{(\phi, \theta, \psi) : |\phi| \leqslant a, |\theta| \leqslant b, |\psi| \leqslant c\}. \tag{16}$$

The dense discrete points in and on the whole solid body should be used together with every discrete position point to compute the inverse kinematics, then to check whether the mechanism at these positions can have the required orientation capabilities by applying all the constraints aforementioned, and to finally obtain all the reachable discrete positions.

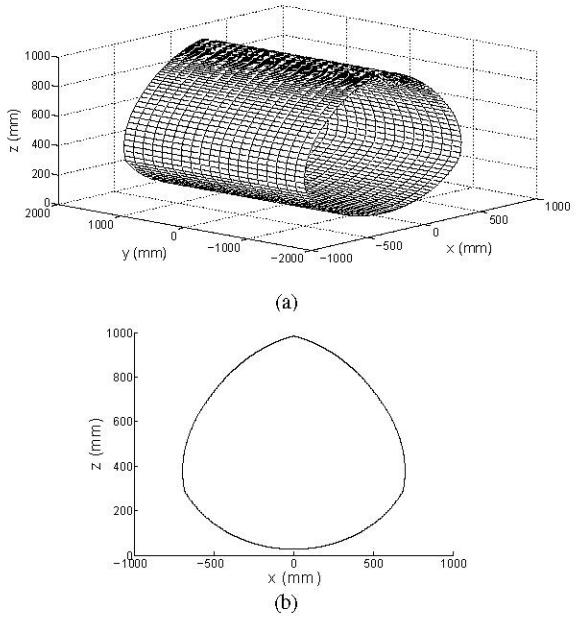

Fig. 3. Workspace of the hexaglide. (a) 3D workspace. (b) XZ cross-section.

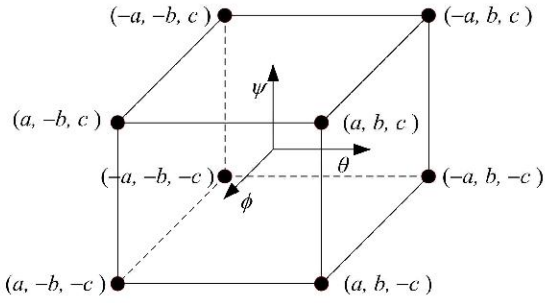

Fig. 4. Orientation requirement as a rectangular solid.

To reduce the computational time, only the six-face boundary of the rectangular solid are checked corresponding to each position. Or even the eight vertexes $(a, b, -c)$, $(a, -b, -c)$, $(a, -b, c)$, $(-a, b, c)$, $(-a, b, -c)$, $(-a, -b, c)$, $(-a, -b, -c)$, (a, b, c) of the rectangular solid are selected and checked as the representative points of the boundary. Although this procedure is not rigorous since, to the best of our knowledge, no reference has performed the relevant justifications, it is effective, or at least an adequate approximation according to the experimental comparisons between checking the whole rectangular solid and checking only its eight vertexes.

Fig. 5(a) shows eight workspace boundaries corresponding to eight vertexes of a rectangular solid ($a = b = c = 10°$), some of which coincide due to the symmetry of the mechanism, and a boundary (the outer-most closed curve) that corresponds to the orientation $(0°, 0°, 0°)$. The area enclosed by and within the eight boundary curves are the set of the reachable positions with the orientation requirement.

As the orientation requirement is increased, the workspace

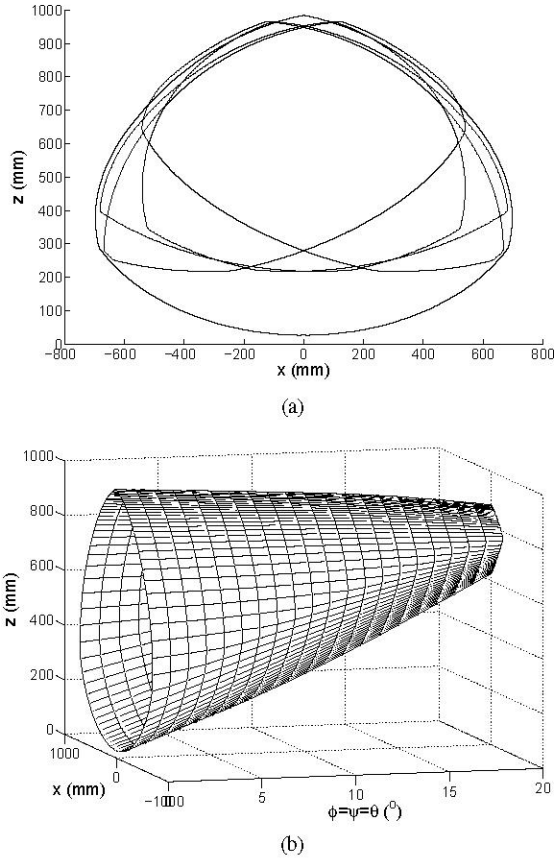

Fig. 5. Workspace with orientation requirements. (a) XZ cross-sections. (b) Workspace influenced by orientation requirements.

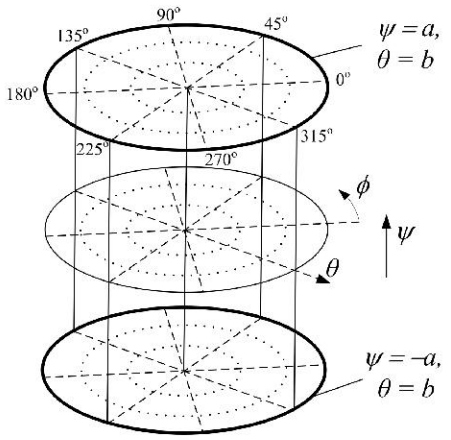

Fig. 6. Orientation requirement as a cylinder.

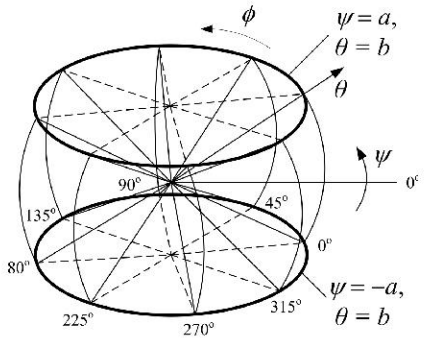

Fig. 7. Orientation requirement as a partial sphere.

decreases in area, as shown in Fig. 5(b).

C. Using Improved Euler Angles with Orientation Requirement as a Cylinder or Partial Sphere

If the improved Euler angles are utilized and the orientation workspace is expressed in a cylindrical coordinate system, the orientation requirement can be represented by a cylindrical solid, which is shown in Fig. 6 and expressed by the following set.

$$W_c = \{(\phi, \theta, \psi) : |\psi| \leqslant a, \theta \in (0°, b], \phi \in [0°, 360°)\}. \quad (17)$$

By the same token regarding the rectangular solid, the cylinder solid can also be represented by its surface or even two circles of a cylinder $\psi = a$, $\theta = b$, $\phi \in [0°, 360°)$ $\psi = -a$, $\theta = b$, $\phi \in [0°, 360°)$.

Besides, if orientation workspace is expressed in a spherical coordinate system, the orientation requirement can be represented by a partial spherical solid in a cylindrical coordinate system, which is illustrated in Fig. 7. And the requirement can also be finally reduced to two circles.

$$W_s = \{(\phi, \theta, \psi) : |\psi| \leqslant a, \theta \in (0°, b], \phi \in [0°, 360°)\}. \quad (18)$$

It can be easily noticed that $W_s = W_c$, so if the reduced orientation requirement of two circles is used, it does not make any difference whether the orientation requirement is expressed in a cylindrical coordinate system or a spherical coordinate system.

The inner closed curve in Fig. 8(a) is the workspace with the orientation requirement $a = b = 10°$. In fact, the two workspace curves corresponding respectively to the two-circle orientation requirement coincide because of the mechanism's symmetry. The outer closed curve is the workspace without any orientation requirement. As the orientation requirement cylinder becomes thicker and higher, the workspace area decreases, as illustrated in Fig. 8(b).

V. Conclusions

This paper presented the potential industrial use of the Hexaglide as a motion simulator for oil tanker trucks, mainly by taking advantage of its merit concerning acceleration along the direction of its rails. To make the workspace more applicable, a new type of workspace was presented, within which, the top plate can attain any of the required ranges of orientation.

This workspace can also be used for workspace optimization. Most current references on parameter optimization of parallel mechanisms are based on the enlargement of position workspace or regard it as one of optimization objectives.

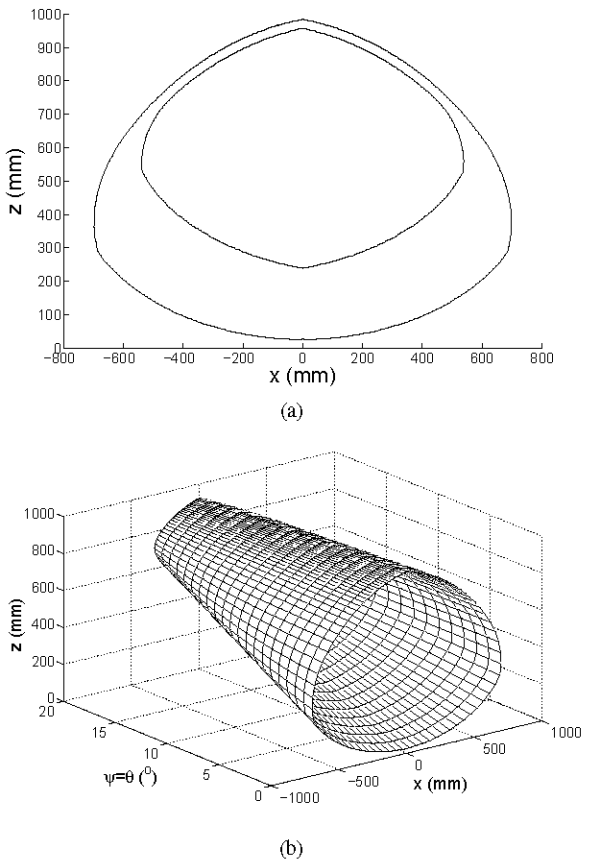

Fig. 8. Workspace with the orientation requirement.(a) XZ cross-sections. (b) Workspace influenced by orientation requirements.

This approach is not practical because a set of parameters resulting in the largest position workspace may probably lead to rather small orientation workspace, since these two kinds of workspace are highly coupled.

ACKNOWLEDGMENT

The authors wish to thank a senior engineer named Gewen Fu for his advice concerning the detailed structure of universal joints, and to acknowledge our debt to the publications listed below.

REFERENCES

[1] J-P. Merlet, *Parallel Robots*, Kluwer Academic Publishers, Dordrecht, The Netherlands, 2000.

[2] B. Dasgupta and T. S. Mruthyunjaya, "The stewart platform manipulator: a review," *Mech. Mach. Theory*, vol. 35, pp. 15–40, 2000.

[3] D. Stewart, "A platform with 6 degrees of freedom," in *Proc. Institution of Mechanical Engineers*, 1965, pp. 371–386.

[4] A. Wiegand, M. Hebsacker, and M. Honegger, "Parallele kinematik und linearmotoren: Hexaglide – ein neues hochdynamisches werkzeugmaschinenkonzept," *Technische Rundschau Transder*, Nr. 25, 1996.

[5] M. Honegger, A. Codourey, and E. Burdet, "Adaptive control of the hexaglide, a 6 dof parallel manipulator," in *Proc. IEEE Int. Conf. Robotics and Automation*, Albuquerque, New Mexico, Apr. 1997, pp. 543–548.

[6] M. Honegger, R. Brega, and G. Schweitzer, "Application of a nonlinear adaptive controller to a 6 dof parallel manipulator," in *Proc. IEEE Int. Conf. Robotics and Automation*, San Francisco, CA, USA, Apr. 2000, pp. 1930–1935.

[7] P. L. Yen, Z. W. Ke, T. S. Lu, and C. W. Lu, "Development of a new safety-enhanced surgical robot using the hexaglide structure," in *Proc. IEEE Int. Conf. System, Man and Cybernetics*, Hague, The Netherlands, Oct. 2004, pp. 2162–2167.

[8] J-P Merlet, "Trajectory verification in the workspace for parallel manipulators," *Int. J. Robotics Res.*, vol. 13, no. 4, pp. 326–333, 1994.

[9] B. Monsarrat and C. M. Gosselin, "Woksapce analyis and optimal design of a 3-leg 6-dof parallel platform mechanism," *IEEE Trans. Robotics and Automation*, vol. 19, no. 6, pp. 954–966, Dec. 2003.

[10] I. A. Bonev and J. Ryu, "Orientation workspace analysis of 6-dof parallel manipulators," in *Proc. ASME Design Engineering Tech. Conf.*, Las Vegas, Nevada, USA, Sept. 1999, pp. 1–8.

[11] I. A. Bonev and J. Ryu, "A new approach to orientation workspace analysis of 6-dof parallel manipulators," *Mech. Mach. Theory*, vol. 36, pp. 15–28, Jan. 2001.

[12] I. A. Bonev and C. M. Gosselin, "Advantages of the modified euler angles in the design and control of pkms," in *Proc. 2002 Parallel Kinematic Machines Int. Conf.*, Chemnitz, Germany, Apr. 2002, pp. 171–188.

[13] T. Huang, J. Wang, and C. M. Gosselin, "Determination of closed form solution for the 2-d orientation workspace of gough-stewart parallel manipulators," *IEEE Trans. Robotics and Automation*, vol. 15, no. 6, pp. 1121–1125, Dec. 1999.

[14] O. Massory and J. Wang, "Workspace evaluation of stewart platforms," in *Proc. ASME Design Engineering Tech. Conf.*, vol. 45, Scottsdale, AZ, Sept. 1992, pp. 337–346.

[15] E. F. Fichter, "A stewart-platform based manipulator: general theory and practical construction," *Int. J. Robotics Res.*, vol. 5, no. 2, pp. 157–182, 1986.

[16] C. M. Gosselin, "Determination of the workspace of 6-dof parallel manipulators," *ASME J. Mech. Des.*, vol. 112, no. 2, pp. 331–337, 1990.

[17] M. Suzuki, K. Watanabe, T. Shibukawa, and K. Hattori, "Development of milling machine with parallel mechanism," *Toyota Tech. Rev.*, vol. 47, no. 1, pp. 125–130, 1997.

[18] Abdul Rauf, Aslam Pervez, and Jeha Ryu, "Experimental results on kinematic calibration of parallel manipulators using a partial pose measurement device," *IEEE Trans. Robotics*, vol. 22, no. 2, pp. 379–384, Apr. 2006.

[19] G. Pritschow and K. H. Wurst, "Systematic design of hexapods and parallel link system," *Ann. CIRP*, vol. 46, no. 1, pp. 291–295, 1997.

[20] A. B. Koteswara Rao, P. V. M. Rao, and S. K. Saha, "Worksapce and dexterity analyses of hexaslides machine tools," in *Proc. IEEE Int. Conf. Robotics and Automation*, Taipei, Taiwan, Sept. 2003, pp. 4104–4109.